Partons and Jets at Strong Coupling from AdS/CFT

Edmond Iancu
Institut de Physique Théorique de Saclay
F-91191 Gif-sur-Yvette, FRANCE

1 Introduction: From RHIC to lattice QCD

Some of the experimental discoveries at RHIC, notably the unexpectedly large medium effects known as elliptic flow and jet quenching, led to the suggestion that the deconfined hadronic matter produced in the intermediate stages of a heavy ion collision is a nearly perfect fluid, so like a strongly coupled plasma. The coupling constant $\alpha_s = g^2/4\pi$ in QCD can never become large, because of asymptotic freedom, but it can be of order one at scales of order $\Lambda_{\rm QCD}$, and this might lead to an effectively strong–coupling behavior. It is notoriously difficult to do reliable estimates in QCD when $\alpha_s \simeq 1$, so it has become common practice to look to the $\mathcal{N} = 4$ supersymmetric Yang–Mills (SYM) theory, whose strong coupling regime can be addressed within the AdS/CFT correspondence [1], for guidance as to general properties of strongly coupled plasmas (see the review papers [2, 3, 4]). Since conformal symmetry is an essential property of $\mathcal{N} = 4$ SYM, this theory is probably not a good model for the dynamics in QCD in the vicinity of the deconfinement phase transition ($T \simeq T_c \simeq 200$ MeV), where the conformal anomaly associated with the running of the coupling in QCD is known to be important. But lattice QCD studies [5] also show that the conformal anomaly decreases very fast with increasing T above T_c and becomes unimportant for temperatures $T \gtrsim 2T_c$ (see Fig. 3 below). Hence, there is a hope that, within the intermediate range of temperatures at $2T_c \lesssim T \lesssim 5T_c$, which is the relevant range for the phenomenology of heavy ion collisions at RHIC and LHC, the dynamics in QCD may be at least qualitatively understood by analogy with $\mathcal{N} = 4$ SYM theory at strong coupling.

Among the most intriguing RHIC data are those referring to *jet quenching*, *i.e.*, the energy loss and the transverse momentum broadening of a relatively 'hard' probe — a heavy and/or energetic quark or lepton, with transverse momentum of a few GeV —, for which one would naively expect a weak–coupling behavior, because of the asymptotic freedom of QCD. Yet, perturbative QCD seems to be unable to explain the strong suppression of particle production in Au+Au collisions, as shown in Fig. 1 (the left figure). Namely, the ratio R_{AA} between the particle yield in Au+Au collisions

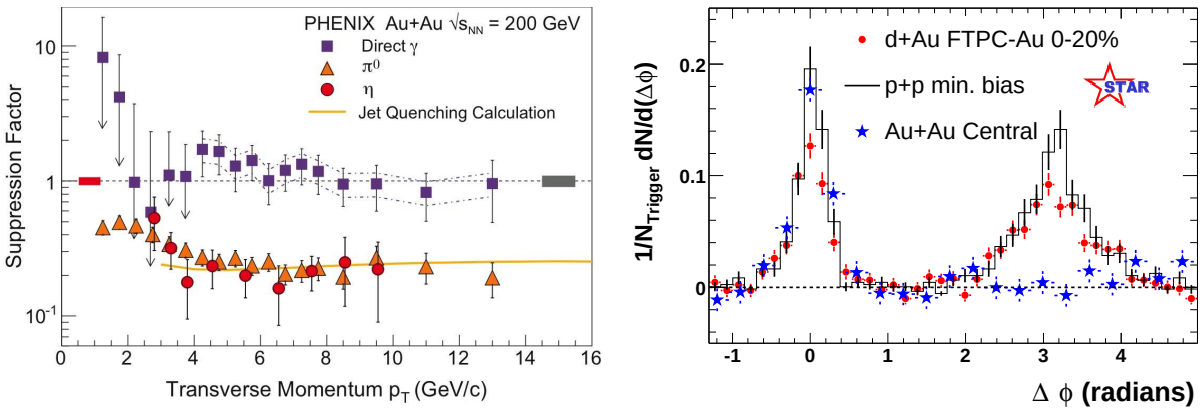

Figure 1: *Left: The ratio R_{AA} of measured versus expected yield of various particles (π^0, η, γ) in Au+Au collisions at $\sqrt{s_{\rm NN}} = 200$ GeV as function of the transverse momentum p_T (RHIC, PHENIX collaboration). Right: Azimuthal correlations for jet measurements at RHIC (STAR collaboration) in p+p, d+Au, and Au+Au collisions.*

and that in p+p collisions rescaled by the number of participants would be one if a nucleus–nucleus collision was the incoherent superposition of collisions between the constituents nucleons of the two incoming nuclei. But the RHIC measurements show that R_{AA} is close to one only for direct photon production, whereas for hadron production it is close to 0.2. This suggests that, after being produced through a hard scattering, the partonic jets are somehow absorbed by the surrounding medium.

Additional evidence in that sense comes from studies of jets, cf. Fig. 1 right. A high–energy proton–proton (or electron–positron) collision generally produces a pair of partons whose subsequent evolution (via fragmentation and hadronisation) leaves two jets of hadrons which propagate back–to–back in the center of mass frame (see Fig. 2 left). Hence, the distribution of the final state radiation w.r.t. the azimuthal angle $\Delta\Phi$ shows two pronounced peaks, at $\Delta\Phi = 0$ and π; this is the curve denoted as 'p+p min. bias' in Fig. 1 right. A similar distribution is seen in deuteron–gold collisions, but not in central Au+Au collisions, where the peak at $\Delta\Phi = \pi$ has disappeared, as shown by the respective RHIC data in Fig. 1 right. It is then natural to imagine that the hard scattering producing the jets has occurred near the edge of the interaction region, so that the near side jet has escaped to the detector, while the away side jet has been absorbed within the medium (see Fig. 2 right).

To conclude, the Au+Au results in Fig.1 show that the matter produced in the intermediate stages of a heavy ion collision is *opaque*, which may well mean that this matter is dense, or strongly–coupled, or both. Besides, the RHIC data on elliptic flow are consistent with theoretical interpretations which assume rapid thermalization (yet another sign of strong interactions !), so one can think of this matter as a quark–gluon plasma in local thermal equilibrium. It is then natural to ask whether one can

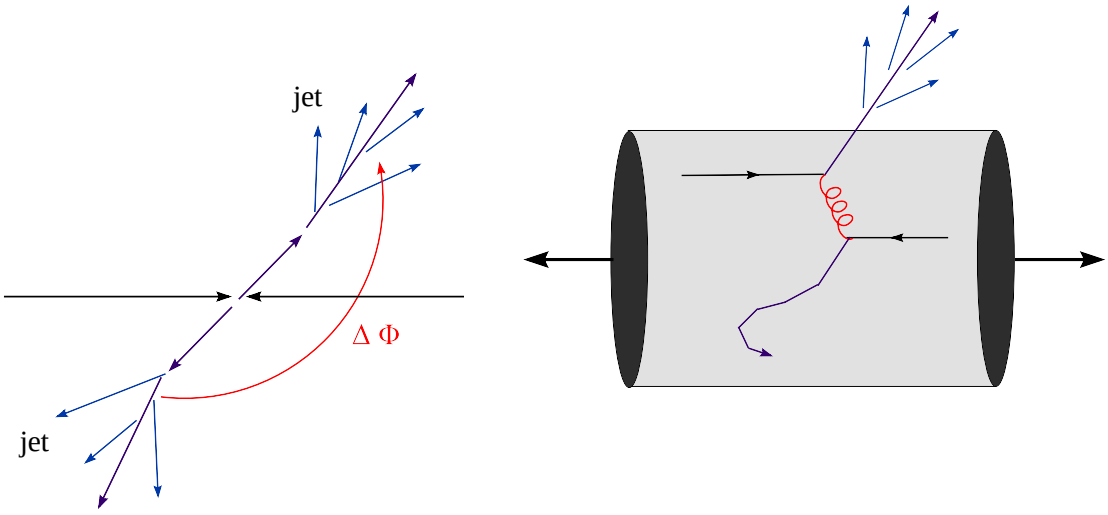

Figure 2: *Jet production in high–energy scattering. Left: a proton–proton collision: the leading partons fragment into two back–to–back hadronic jets, which are seen by the detector. Right: a nucleus–nucleus collision: one of the leading partons escapes the interaction region and enters the detector, but the other one is absorbed in the surrounding matter.*

discriminate between weak coupling and strong coupling behavior on the basis of the lattice results for the QCD thermodynamics. Unfortunately however the theoretical interpretation of these results is not totally free of ambiguities, as we now explain.

Figure 3 exhibits the lattice results for the conformal anomaly $(\epsilon - 3p)/T^4$ (left) and for the pressure p (right) in units of T^4. The left figure confirms that the QCD plasma is nearly conformal for temperatures $T \gtrsim 2T_c$: after showing a peak at the deconfinement phase transition, the relative conformal anomaly $(\epsilon - 3p)/\epsilon$ decreases very fast with increasing T and becomes smaller than 10% when $T \gtrsim 2T_c$. The right figure shows that, after a rapid jump at the phase transition, the pressure slowly approaches the respective ideal gas limit p_0, in such a way $p/p_0 \simeq 0.85$ at $T = 3T_c$. This deviation from the ideal gas is rather small, of the order of the first perturbative correction $\mathcal{O}(\alpha_s)$, and indeed perturbation theory in QCD at finite temperature does a good job in reproducing the lattice results for temperatures $T \gtrsim 2.5T_c$, as shown by the 'HTL' band in that figure [7]. (This is shown here for the pure glue SU(3) gauge theory, but a similar agreement holds for QCD with nearly massless quarks.) On the other hand, this value $p/p_0 \simeq 0.85$ is not too far from the respective result in the strong–coupling limit of $\mathcal{N} = 4$ SYM, as inferred via AdS/CFT, and which reads $p/p_0 = 0.75$ [1]. Thus, although fully consistent with weak coupling expectations (a tendency which is even more visible in the recent lattice results for quark number susceptibilities [5]), the lattice result do not fully exclude a strong–coupling behavior in the QCD plasma for temperatures $2T_c \lesssim T \lesssim 5T_c$.

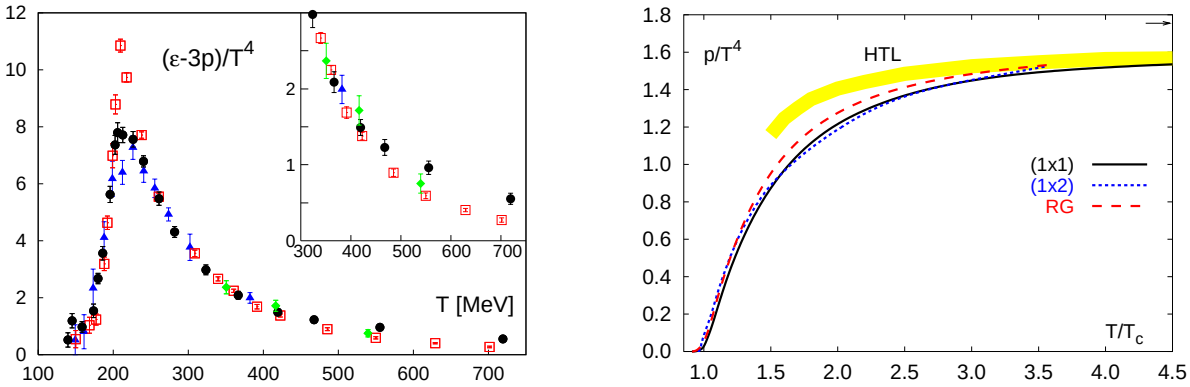

Figure 3: *Lattice results for the QCD trace anomaly, $T^\mu_\mu = \epsilon - 3p$ (left) [5] and for the pressure of the SU(3) gauge theory (right) [6]. In the right figure, different lines correspond to different gauge actions, whereas the upper band denoted as 'HTL' (for 'Hard Thermal Loop') represents the results of a parameter–free resummation of perturbation theory [7]. The small arrow in the upper right corner indicates the pressure of an ideal gas.*

2 A lattice test of the coupling strength in QCD

If the lattice results for the QCD thermodynamics cannot unambiguously distinguish between weak and strong coupling behavior, is there any other way how one could test the strength of the coupling in lattice QCD at finite temperature ? In what follows, we shall describe a recent proposal in that sense [8], which involves the lattice measurement of leading–twist operators. These are the operators with spin n, classical dimension $d = n + 2$, and twist $t = d - n = 2$, which in the weak coupling regime control the operator product expansion (OPE) of deep inelastic scattering (DIS) at large photon virtuality Q^2 [9]. There are two infinite sequences of leading–twist operators — the fermionic ones and the gluonic ones — among which we only show here those with $n = 2$ (see, e.g., [9] for the general expressions) :

$$\mathcal{O}_f^{\mu\nu} \equiv \frac{1}{2}\,\overline{q}\big(\gamma^\mu i D^\nu + \gamma^\nu i D^\mu\big) q\,, \tag{1}$$

(the sum over quark flavors is implicit and we neglect the quark masses) and

$$\mathcal{O}_g^{\mu\nu} \equiv -F_a^{\mu\alpha} F_\alpha^{\nu,a} + \frac{1}{4}\, g^{\mu\nu} F_a^{\alpha\beta} F^a_{\alpha\beta}\,. \tag{2}$$

These are operators recognized as the energy–momentum tensors for quarks and gluons, respectively. More generally, the hadron expectation values of the spin–n leading–twist operators measure the $(n-1)$–th moment of the longitudinal momentum fraction carried by the quark and gluon constituents of that hadron.

Being composite, these operators are well defined only with a renormalization prescription, and thus implicitly depend upon the renormalization scale Q^2. Physically, this dependence expresses the fact that quantum fields can radiate and their internal structure in terms of 'bare' quanta depends upon the resolution scale Q^2 at which one probes this structure.

For instance, the success of the valence parton model for high–energy scattering in QCD is deeply related to the asymptotic freedom property of QCD. This property guarantees that parton branching at $Q^2 \gg \Lambda^2_{\rm QCD}$ is controlled by weak coupling, via the bremsstrahlung process. This in turn favors the emission of 'soft' and 'collinear' quanta, *i.e.* quanta which carries only a small fraction x of the longitudinal momenta of their parent partons and relatively small transverse momenta. Hence, although there are many small–x gluons in the proton wavefunction at high energy, most of the proton longitudinal momentum is still carried by the point–like valence quarks.

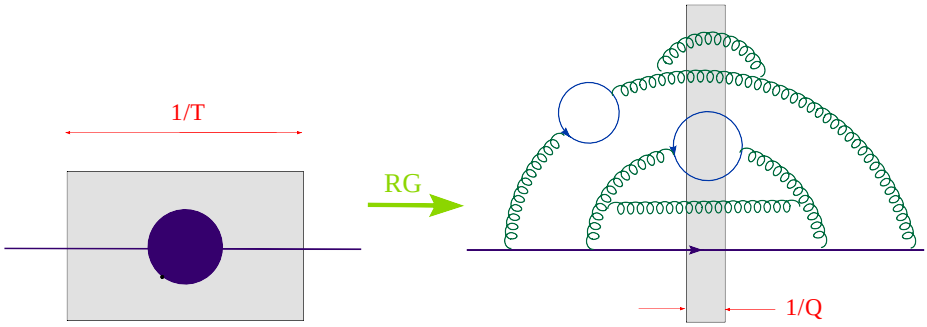

Figure 4: *Parton evolution from the thermal scale T up to the harder scale $Q \gg T$.*

By contrast, at strong coupling one expects parton branching to be fast and 'quasi–democratic' — the energy of the parent parton is quasi equally shared by the daughter partons —, so the partons will rapidly cascade down to low–momentum constituents [10, 11, 12]. At finite temperature, it is natural to assume that the branchings have taken place between the temperature scale T and the "hard" resolution scale Q, with $Q \gg T$, at which the operator is evaluated (see Fig. 4). Hence, although there is in principle no contradiction in having a quasiparticle picture for a strongly–coupled plasma on the thermal scale T (as shown by the similarity between the strong–coupling and, respectively, zero–coupling results for the entropy density of the $\mathcal{N} = 4$ SYM plasma [1]), one expects these 'quasiparticles' to be highly composite, without a pointlike core carrying a significant fraction of the quasiparticle energy.

These physical considerations find a precise mathematical expression in the renormalization group equations describing the evolution of the leading–twist operators with the resolution scale μ^2. Up to operator mixing issues to which we shall return

in a moment, these equations read (for a generic spin–n operator $\mathcal{O}^{(n)}$)

$$\mu^2 \frac{\mathrm{d}}{\mathrm{d}\mu^2}\,\mathcal{O}^{(n)} \,=\, \gamma^{(n)}\mathcal{O}^{(n)} \quad \Longrightarrow \quad \frac{\mathcal{O}^{(n)}(Q^2)}{\mathcal{O}^{(n)}(\mu_0^2)} \,=\, \exp\left\{\int\limits_{\mu_0^2}^{Q^2} \frac{\mathrm{d}\mu^2}{\mu^2}\,\gamma^{(n)}(\mu^2)\right\}, \tag{3}$$

where $\gamma^{(n)}$ is the corresponding anomalous dimension and is strictly negative — meaning that the evolution increases the number of partons with small longitudinal momentum fraction x while decreasing that of the partons with large x —, except for the total energy–momentum operator

$$T^{\mu\nu} \,=\, \mathcal{O}_f^{\mu\nu} \,+\, \mathcal{O}_g^{\mu\nu}\,, \tag{4}$$

which has zero anomalous dimension since it is a conserved quantity (and hence it does not depend upon the resolution scale Q^2). Hence, in the continuum limit $Q^2 \to 0$, the expectation values of all the leading–twist operator except for T must vanish. But the rate of this evolution is very different at weak and respectively strong coupling.

`(i) Weak coupling :` To lowest order in the running coupling, one has

$$\gamma^{(n)}(\mu^2) \,=\, -a^{(n)}\,\frac{\alpha_s(\mu^2)}{4\pi} \quad \Longrightarrow \quad \frac{\mathcal{O}^{(n)}(Q^2)}{\mathcal{O}^{(n)}(\mu_0^2)} \,=\, \left[\frac{\ln(\mu_0^2/\Lambda^2)}{\ln(Q^2/\Lambda^2)}\right]^{a^{(n)}/b_0}\,, \tag{5}$$

with $\alpha_s(\mu^2) = 4\pi/[b_0 \ln(\mu^2/\Lambda^2)]$, $\Lambda \equiv \Lambda_{\rm QCD} \approx 200$ MeV, $b_0 = (11N_c - 2N_f)/3$, and $a^{(n)} > 0$. Thus, the perturbative evolution is rather slow — merely logarithmic.

`(ii) Strong coupling & conformal field theory :` At strong coupling, direct calculations in QCD are not possible anymore, but we shall use the corresponding results for $\mathcal{N} = 4$ SYM as a hint towards what could be the behavior in QCD in such a strong–coupling scenario. In a conformal field theory, $\gamma^{(n)}$ is scale–independent and negative (with the exception of $T^{\mu\nu}$, of course), so the evolution is power–like:

$$\frac{\mathcal{O}^{(n)}(Q^2)}{\mathcal{O}^{(n)}(\mu_0^2)} \,=\, \left[\frac{\mu_0^2}{Q^2}\right]^{|\gamma^{(n)}|}\,. \tag{6}$$

Moreover, AdS/CFT predicts that, at strong coupling $\lambda \equiv g^2 N_c \gg 1$, all the non–zero anomalous dimensions are very large $|\gamma^{(n)}| \sim \mathcal{O}(\lambda^{1/4})$ [13], hence the leading–twist operators rapidly die away with increasing Q^2 (meaning that all partons have fallen down to small values of x). In particular, the DIS structure functions at strong coupling are controlled by $T^{\mu\nu}$ together with protected higher–twist operators which have zero anomalous dimensions [10].

These results suggest that a natural way to measure the strength of the coupling in QCD at finite temperature is to compute thermal expectation values of leading–twist operators in lattice QCD [8]. These operators evolve from the natural physical scale

T up to the resolution scale Q set by the lattice spacing: $Q = a^{-1}$. In practice, the ratio $Q/T = aT$ is not very large, $Q/T \lesssim 10$, so if the evolution is perturbative, cf. Eq. (5), the expectation value of an unprotected operator is only slightly reduced — by a few percent. On the other hand, if the plasma is effectively strongly coupled at the scale T, than at least the early stages of the evolution (say from the scale T up to an intermediate scale $\mu \approx$ a few times T) should involve a large negative anomalous dimension, leading to a strong suppression in the expectation value measured at the final scale Q.

The previous argument applies to the unprotected operators, which include all the higher–spin operators with $n \geq 4$. Unfortunately, however, it turns out that it is very difficult, if not impossible, to accurately measure on the lattice such high–spin operators. There is another possibility, though, which should be easier in practice: this is to measure the linear combination of the spin–2 operators in Eqs. (1)–(2) which is orthogonal to $T^{\mu\nu}$ within the renormalization flow and therefore has a non–zero, and negative, anomalous dimension. There is however a serious problem with this proposal too: finding the proper orthogonal contribution requires the knowledge of the relevant anomalous dimensions, which in full QCD are computable only in perturbation theory, and hence at weak coupling.

Fortunately, there is a simpler version of the theory where the identification of this operator becomes possible for any value of the coupling: this is *quenched* QCD. Loosely speaking, this is the theory obtained from QCD after removing all the quark loops. On the lattice, this is non–perturbatively defined by removing the fermionic determinant from the QCD action. Note that the quark fields are still present in this theory, but only as external probes. As argued in Ref. [8], $\mathcal{O}_f^{\mu\nu}$ is the operator orthogonal to $T^{\mu\nu}$ in quenched QCD. Indeed, in quenched QCD, a quark can emit gluons, but the emitted gluons, as well as those from the thermal bath, are not allowed to emit quark–antiquark pairs. Hence, when the system is probed on a sufficiently hard scale, most of the total energy appears in the gluon fields. In the continuum limit, the total energy–momentum tensor reduces to its gluonic component: $T^{\mu\nu} \to \mathcal{O}_g^{\mu\nu}(Q^2)$ as $Q^2 \to \infty$.

To summarize, the proposal made in Ref. [8] is to measure the thermal expectation value $\langle \mathcal{O}_f^{00}(Q^2) \rangle_T$ of the quark energy density in lattice quenched QCD, for a temperature $T = 2T_c \simeq 600$ MeV and for an inverse lattice spacing $Q = a^{-1} \simeq 8T$. If the deviation from the corresponding result for the ideal Fermi–Dirac gas turns out to be relatively small, $\lesssim 30\%$, then one can conclude that the QCD plasma is weakly coupled at the scale T. If on the other hand the lattice result turns out to be considerably smaller, then there must be a regime in μ around T where QCD is effectively strongly coupled. Simple estimates together with the RHIC phenomenology of jet quenching suggest that a suppression by a factor of 5 could be expected in the strong–coupling scenario [8].

3 DIS and parton saturation at strong coupling

The previous discussion emphasized the importance of understanding parton evolution at strong coupling. The OPE together with the renormalization group provides a valuable tool in that sense, but this applies only for sufficiently large Q^2 — where it teaches us that, at strong coupling, the partons disappear through branching — and thus it cannot tell us what is the final fate of these partons, after cascading down to lower momenta. In particular, this is inappropriate to study the unitarity corrections to scattering at high energy. Fortunately, the gauge/string duality also allows us to directly compute the cross–sections for elementary processes, with results which shed further light on the parton evolution at strong coupling [3, 4, 10, 11, 12, 14].

The simplest version of the formalism, known as the 'supergravity approximation', is obtained by taking the large–N_c limit, or, equivalently, the large 't Hooft coupling limit: $\lambda = g^2 N_c \to \infty$ with g fixed and small ($g \ll 1$). This is generally not a good limit to study a scattering process, since the corresponding amplitude is suppressed as $1/N_c^2$ [10, 11], yet it is meaningful for processes taking place in a deconfined plasma, like those of interest for heavy ion physics: indeed, the plasma involves N_c^2 degrees of freedom per unit volume, thus yielding finite amplitudes when $N_c \to \infty$. In this limit, the $\mathcal{N} = 4$ SYM plasma at finite temperature is described as a 'black–hole' (more properly, a black–brane) embedded in AdS_5 and the dynamics reduces to classical gravity in this curved space–time [1, 2, 3, 4]. It should be emphasized that the black hole (BH) is homogeneous in the physical 4 dimensions[1], so like the plasma that is it dual to, but it has an horizon in the radial, or 'fifth', dimension of AdS_5, at a position which is determined by the temperature of the plasma.

The AdS_5 BH geometry is illustrated in Fig. 5, which also shows the supergravity process dual to DIS off the $\mathcal{N} = 4$ SYM plasma: A space–like virtual photon, with 4–momentum $q^\mu = (\omega, 0, 0, q)$ and virtuality $Q^2 \equiv q^2 - \omega^2 \gg T^2$, acts as a perturbation on the Minkowski boundary of AdS_5 ($\chi = 0$), thus inducing a massless, vector, supergravity field A_m (with $m = \mu$ or χ) which propagates within the bulk of AdS_5 ($\chi > 0$), according to the Maxwell equations in curved space–time:

$$\partial_m\big(\sqrt{-g}g^{mp}g^{nq}F_{pq}\big) \,=\, 0\,, \qquad \text{where} \quad F_{mn} = \partial_m A_n - \partial_n A_m\,. \tag{7}$$

Here, g^{mn} is the metric tensor in 5–dimensions which in particular contains the information about the BH horizon at $\chi = 1/T$ (we follow the conventions in [3]). Thus Eq. (7) describes the gravitational interaction between the Maxwell field A_m and the BH. As usual, the strength of this interaction is proportional to the product $\omega^2 T^4$ between the energy densities in the two interacting systems — the virtual photon and the plasma. Interestingly, there is a threshold value for this quantity, of order Q^6,

[1] More recently, a finite–length plasma 'slice' has been considered too, as a model for a nucleus which admits a simple supergravity dual (a 'shockwave') [15].

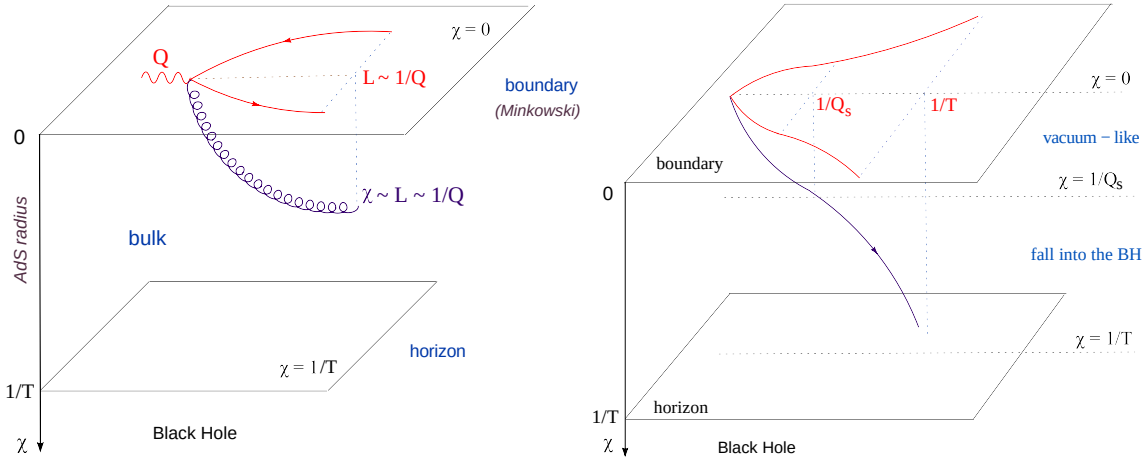

Figure 5: *Space–like current in the plasma: the trajectory of the wave packet in AdS_5 and its 'shadow' on the boundary. Left: low energy — the Maxwell wave gets stuck near the boundary up to tunnel effect. Right: high energy — the wave falls into the BH.*

below which there is essentially no interaction [12]: so long as $\omega T^2 \ll Q^3$, the Maxwell wave is stuck within a distance $\chi \lesssim 1/Q \ll 1/T$ from the Minkowski boundary and does not 'see' the BH (cf. Fig. 5 left). But for higher energies and/or temperatures, such that $\omega T^2 \gtrsim Q^3$, the wave gets attracted by the BH and eventually falls into the latter. Physically, this means that the energetic space–like photon is absorbed with probability one into the plasma — the 'black disk limit' for DIS (cf. Fig. 5 right).

This critical value $Q_s \sim (\omega T^2)^{1/3}$, together with the physical picture of the scattering, can be understood with the help of the 'UV/IR correspondance', which relates the 5th dimension of AdS_5 to the momenta (or typical sizes) of the quantum fluctuations which are implicitly integrated out in the boundary gauge theory. Namely, the radial penetration χ of the Maxwell wave packet in AdS_5 is proportional to the transverse size L of the quantum fluctuation of the virtual photon in the dual gauge theory. By the uncertainty principle, we expect a highly energetic space–like photon with $\omega \simeq q \gg Q$ to fluctuate into a partonic system with transverse size $L \sim 1/Q$ — which indeed matches the radial penetration of the dual Maxwell field, as illustrated in Fig. 5 left — and a finite lifetime $\Delta t \sim \omega/Q^2$. The space–like fluctuation cannot decay into on–shell partons (at least, not in the vacuum), because of energy–momentum conservation. But the situation can change in the presence of the plasma. Unlike the photon, which is color neutral, its partonic fluctuation has a dipolar color moment and thus can interact with the plasma. Via such interactions, the partons can acquire the energy and momentum necessary to get on–shell, and then the fluctuation decays: the space–like photon disappears (cf. Fig. 5 right).

Let us now return to the threshold value $Q_s \sim (\omega T^2)^{1/3}$, to which we shall refer

as the *saturation momentum*. The condition $Q \sim Q_s$ can be rewritten as

$$Q \sim \frac{\omega}{Q^2} T^2 , \tag{8}$$

which admits the following interpretation [12] : the scattering becomes strong when the lifetime $\Delta t \sim \omega/Q^2$ of the partonic fluctuation is large enough for the mechanical work $W = \Delta t \times F_T$ done by the *plasma force* $F_T \sim T^2$ acting on these partons to compensate for the energy deficit Q of the space–like system. This plasma force $F_T \sim T^2$ represents the effect of the strongly–coupled plasma on color dipole fluctuations and can be viewed as a prediction of the AdS/CFT calculation.

Introducing the Bjorken x variable $x \equiv Q^2/(2\omega T)$ for DIS off the plasma — as usual, this has the meaning of the longitudinal momentum fraction of the plasma constituent which absorbs the virtual photon —, one can rewrite the plasma *saturation line* as $Q_s(x) = T/x$ or, alternatively, $x_s(Q) = T/Q$. The AdS/CFT results then suggest a partonic picture for the strongly–coupled plasma [12]. For $Q \gg Q_s(x)$ (or, equivalently, $x \gg x_s(Q)$), the scattering is negligible and the DIS structure function F_2 is exponentially small: $F_2(x, Q^2) \sim \exp\{-Q/Q_s(x)\}$. This shows that there are no pointlike constituents in the strongly coupled plasma, in agreement with the OPE argument in Sect. 2. For $x \lesssim x_s(Q)$, on the other hand, the scattering is maximal and the structure function is found to be large: $F_2(x, Q^2) \sim x N_c^2 Q^2$. This is in agreement with our physical expectation that partons must somehow accumulate at small values of x, as a result of branching, and is moreover consistent with energy–momentum conservation, which requires the integral $\int_0^1 \mathrm{d}x\, F_2(x, Q^2)$ to have a finite limit as $Q^2 \to \infty$ [9]. The previous results imply indeed

$$\int_0^1 \mathrm{d}x\, F_2(x, Q^2) \simeq x_s F_2(x_s, Q^2) \sim N_c^2 T^2 , \tag{9}$$

where the integral is dominated by $x \simeq x_s(Q)$: the energy and momentum of the plasma as probed on a 'hard'resolution scale $Q^2 \gg T^2$ is fully carried by the partons 'along the saturation line', *i.e.*, those having $x \simeq T/Q$. A similar picture holds for other hadronic targets so like a 'glueball' [10, 11] or a 'nuclear' shockwave [15], but the respective saturation momentum rises slower with $1/x$ than for the infinite plasma: $Q_s^2(x) \propto 1/x$ for a finite–size 'hadron' as opposed to $Q_s^2(x) \propto 1/x^2$ for the plasma. The additional factor $1/x$ in the case of the plasma comes from the lifetime $\Delta t \sim \omega/Q^2 \sim 1/xT$ of the partonic fluctuation: since the medium is infinite, the effects of the scattering accumulate all the way along the parton lifetime.

4 High–energy scattering and hard probes

The parton picture at strong coupling as just described has some striking physical consequences for the high–energy scattering problem which look very different from

our experience with QCD. For instance, the rapid energy growth $Q_s^2(x) \propto 1/x$ of the saturation momentum, which is automatic in this gravity context, is much faster than the respective growth observed in the HERA data, namely $Q_s^2 \sim 1/x^\omega$ with $\omega \simeq 0.2 \div 0.3$, and which is in fact well accounted for by perturbative QCD [16]. Also, the absence of large–x partons in a hadronic wavefunction at strong coupling means that, in a hypothetical scattering between two such hadrons, there would be no particle production at either forward or backward rapidities: the two nuclei colliding with each other at strong coupling would fully stop each other [17]. This is in sharp contrast to the situation at RHIC, where the large–x partons from the incoming nuclei are seen to emerge from the collision, as hadronic jets, along their original trajectories.

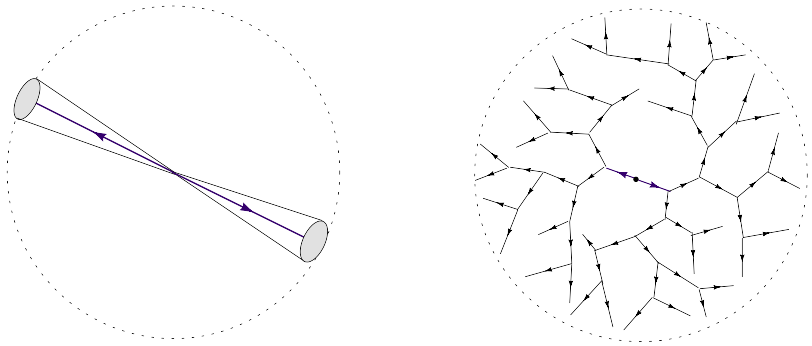

Figure 6: *Final state in e^+e^- annihilation. Left: weak coupling. Right: strong coupling.*

A related, but perhaps even more striking (in view of its obvious conflict with real–life QCD) prediction of AdS/CFT is the absence of jets in electron–positron annihilation at strong coupling [12, 14]. Fig. 6 exhibits the typical, 2–jet, final state in e^+e^- annihilation at weak coupling (left) together with what should be the corresponding state at strong coupling (right). In both cases, the final state is produced via the decay of a time–like photon into a pair of partons and the subsequent evolution of this pair. At weak coupling this evolution is rather slow and consists mostly in the emission of soft and collinear gluons, with the result that the leading partons get dressed into a pair of well–collimated jets of hadrons (cf. Fig. 6 left). Multi–jet ($n \geq 3$) events are possible as well, but they have a lower probability (which is computable in pQCD), as they require hard parton emissions in the final state, which are suppressed by asymptotic freedom [9]. At strong coupling, on the other hand, parton branching is much more efficient, as previously explained: all splittings are hard and happen very fast, so they rapidly split the original energy over many quanta which carry energies and momenta of the order of the soft, confinement, scale, and which are almost isotropically distributed in space, because of their large number. Thus, the respective final state shown no sign of jets, but only an isotropic distribution of hadronic matter (cf. Fig. 6 right) [14].

Let us finally return to our original motivation for studying the dynamics at strong coupling, which was the propagation of a 'hard probe' through a strongly–coupled plasma. Consider the energy loss by a heavy quark towards the plasma: the respective AdS/CFT calculation has been given in [18], but the result can be also inferred from the previously explained parton picture at strong coupling [20]. Among the virtual, space–like, quanta which are continuously emitted and reabsorbed by the heavy quark, only those can escape to the plasma which have a virtuality Q lower than the plasma saturation momentum $Q_s(x)$ for a value of x set by the lifetime of the fluctuation: $1/x \sim T\Delta t$ with $\Delta t \sim \omega/Q^2$. Since $\mathrm{d}E/\mathrm{d}t \propto \omega/\Delta t \sim Q^2$, the energy loss is controlled by the fluctuations having the maximal possible value for the virtuality, that is, those having $Q \sim Q_s(x)$ with x set by the rapidity γ of the heavy quark. Using $\gamma = \omega/Q$ and $Q_s \sim T/x \sim \gamma T^2/Q_s$, one finds $Q_s \sim \sqrt{\gamma}T$ and hence

$$-\frac{\mathrm{d}E}{\mathrm{d}t} \simeq \sqrt{\lambda}\,\frac{\omega}{(\omega/Q_s^2)} \simeq \sqrt{\lambda}\,Q_s^2 \sim \sqrt{\lambda}\,\gamma\,T^2\,, \tag{10}$$

where the factor $\sqrt{\lambda}$ enters via the normalization of the Nambu-Goto action and expresses the fact that, at strong coupling, the heavy quark does not radiate just a single quanta per time Δt, but rather a large number $\sim \sqrt{\lambda}$. Eq. (10) is parametrically consistent with the respective AdS/CFT result [18]. Note the strong enhancement of the medium effects at high energy, as expressed by the Lorentz γ factor in the r.h.s of (10): this is in qualitative agreement with the strong suppression of particle production seen in Au+Au collisions at RHIC, but one should be very careful before directly comparing such AdS/CFT results with the QCD phenomenology.

Consider similarly the momentum broadening: the $\sqrt{\lambda}$ quanta emitted during a time interval Δt are uncorrelated with each other, so their transverse momenta are randomly oriented and the cumulating recoils increase the *squared* transverse momentum of the heavy quark (while its *average* momentum remains of course unchanged)

$$\frac{\mathrm{d}\langle p_\perp^2\rangle}{\mathrm{d}t} \sim \frac{\sqrt{\lambda}\,Q_s^2}{(\omega/Q_s^2)} \sim \sqrt{\lambda}\,\frac{Q_s^4}{\gamma Q_s} \sim \sqrt{\lambda}\,\sqrt{\gamma}\,T^3\,, \tag{11}$$

which is parametrically the same as the respective AdS/CFT results in Refs. [19].

To summarize, the strong–coupling picture of high–energy scattering appears to be very different from everything we know, theoretically and experimentally, about real–life QCD. There are no valence partons, the saturation momentum (and hence the hadronic cross–sections) grow much too fast with increasing energy, and there are no jets in the final state. This is not necessarily a surprise: within QCD, these high–energy phenomena are controlled by hard momentum exchanges and thus by weak coupling, by virtue of the asymptotic freedom. On the other hand, AdS/CFT might give us some qualitative insight in the semi–hard physics of particle production in heavy ion collisions, and also in some longstanding problems like thermalization and the emergence of hydrodynamics in the late stages of such a collision.

References

[1] O. Aharony, S. S. Gubser, J. M. Maldacena, H. Ooguri, and Y. Oz, "Large N field theories, string theory and gravity", *Phys. Rept.* **323** (2000) 183.

[2] D. T. Son and A. O. Starinets, *Ann. Rev. Nucl. Part. Sci.* **57** (2007) 95,

[3] E. Iancu, *Acta Phys. Polon.* **B39** (2008) 3213, `arXiv:0812.0500 [hep-ph]`.

[4] S. S. Gubser, S. S. Pufu, F. D. Rocha, and A. Yarom, "Energy loss in a strongly coupled thermal medium and the gauge-string duality," `arXiv:0902.4041`.

[5] M. Cheng *et al.*, *Phys. Rev.* **D77** (2008) 014511; *Phys. Rev.* **D79** (2009) 074505.

[6] F. Karsch, E. Laermann and A. Peikert, *Phys. Lett.* **B 478** (2000) 447.

[7] J.-P. Blaizot, E. Iancu, A. Rebhan, *Phys. Rev.* **D63** 065003 (2001).

[8] E. Iancu and A. H. Mueller, `arXiv:0906.3175 [hep-ph]`.

[9] M. E. Peskin and D. V. Schroeder, "An Introduction to quantum field theory,". Reading, USA: Addison-Wesley (1995) 842 p.

[10] J. Polchinski and M. J. Strassler, *JHEP* **05** (2003) 012.

[11] Y. Hatta, E. Iancu, A. H. Mueller, *JHEP* **01** (2008) 026.

[12] Y. Hatta, E. Iancu, A. H. Mueller, *JHEP* **01** (2008) 063; *JHEP* **05** (2008) 037.

[13] S. S. Gubser, I. R. Klebanov, A. M. Polyakov, *Nucl. Phys.* **B636** (2002) 99.

[14] D. M. Hofman and J. Maldacena, *JHEP* **05** (2008) 012.

[15] A. H. Mueller, A. I. Shoshi, B.-W. Xiao, *Nucl. Phys.* **A822** (2009) 20; E. Avsar, E. Iancu, L. McLerran, D. N. Triantafyllopoulos, `arXiv:0907.4604 [hep-th]`.

[16] E. Iancu, Nucl. Phys. Proc. Suppl. **191** (2009) 281, `arXiv:0901.0986 [hep-ph]`.

[17] J. L. Albacete, Y. V. Kovchegov, A. Taliotis, *JHEP* **0807** (2008) 100.

[18] C. P. Herzog, A. Karch, P. Kovtun, C. Kozcaz, L. G. Yaffe, *JHEP* **0607** (2006) 013; S. S. Gubser, *Phys. Rev.* **D 74** (2006) 126005.

[19] J. Casalderrey-Solana, D. Teaney, *Phys. Rev.* **D 74** (2006) 085012; *JHEP* **04** (2007) 039; S. S. Gubser, *Nucl. Phys.* **B790** (2008) 175.

[20] F. Dominguez, C. Marquet, A. H. Mueller, B. Wu, B. W. Xiao, *Nucl. Phys.***A811** (2008) 197; G. C. Giecold, E. Iancu, A. H. Mueller, *JHEP* **0907** (2009) 033.